Coherent control of the refractive index using optical bistability

H. Aswath Babu and Harshawardhan Wanare*
Department of Physics, Indian Institute of Technology, Kanpur 208 016, India
(Received 6 September 2012; published 19 March 2013)

Refractive index and absorption experienced by a probe field propagating through a three-level atomic medium can be effectively manipulated by the bistable behavior of a control field. The probe field couples the lower transition of the atom in a ladder configuration and experiences normal or anomalous dispersion depending on the control field being in the upper or lower bistable state, respectively. We also obtain nonlinear dynamical instability in the form of periodic self-pulsing as the lower bistable branch becomes unstable, quite unlike earlier demonstrations of an unstable regime in the upper branch. Consequently, the susceptibility experienced by the probe field varies periodically in time as dictated by the control field self-pulsing.

DOI: 10.1103/PhysRevA.87.033821 PACS number(s): 42.65.Pc, 32.80.Qk, 42.50.Nn, 42.65.Sf

I. INTRODUCTION

Interaction of light with matter in the linear regime is completely determined by the refractive index and absorption of the material. In the past two decades these few ubiquitous quantities have been engineered coherently in a wide variety of ways, resulting in exciting phenomena such as slow light [1], superluminal light [2], making a resonant absorbing medium transparent with electromagnetically induced transparency (EIT) [3], achieving giant enhancement in the refractive index [4], coherently controllable metamaterials [5], and many such developments that have transformed the practice of present day optics. Recently, coherent control of the refractive index and spatially varying refractive index accompanied by negligible absorption have also been proposed [6,7]. The control of optical bistability (OB) using coherent interactions supplementing the bistable field has been in vogue for a few years now [8,9]. Recently, we have also predicted the existence of a negative hysteresis bistable response in a three-level atom experiencing double feedback along two adjacent transitions [10], and a host of nonlinear dynamical behavior such as self-pulsing and chaos [11]. Nonlinear dynamics in driven OB systems involving a three-level Λ system in the EIT regime has been studied earlier [12,13]. In this paper, we present another mechanism that allows an effective manipulation of the refractive index using OB, varying from anomalous to normal as well as time-dependent periodic susceptibility (absorption and refractive index). This is achieved through the cooperative effect at an adjacent transition exhibiting OB. However, our system does not rely on the EIT effect for the control mechanism.

The refractive index governs the frequency-dependent phase delay experienced by the electromagnetic field in the medium, whereas the absorption coefficient its extinction. The Kramers-Kronig relation based on *causality* relates the spectral dependence of the refractive index to the associated absorption, therefore it is impossible to vary exclusively only the refractive index or the absorption without affecting the other. The manipulation of the refractive index and absorption through control field OB could be used to control the propagation of the probe field through the medium. We demonstrate that for the bistable field in the ON state (a large intracavity field associated with the upper branch of the S-shaped OB response [14]) the probe field experiences normal dispersion accompanied with negligible absorption. In contrast, the bistable field in the OFF state (a weak intracavity field associated with the lower cooperative branch) leads to anomalous dispersion and the associated absorption. In optical communication, apart from being a switch [15], OB can also provide an excellent handle to either delay the probe pulse through normal dispersion or advance it through anomalous dispersion. Furthermore, we propose a scheme of realizing periodically varying susceptibility for the probe field by creating control field instability in the lower branch of OB. This instability occurs for a single-mode OB field at intensities much lower than those required to saturate the atom. The creation of instability assisted by atomic coherence leads to nonlinear dynamical effects, such as self-pulsing whose period and amplitude can be tuned to obtain a range of time scales for the susceptibility.

Earlier studies of instability in OB systems range from the Ikeda instability [16] in two-level OB systems [17] to three-level driven OB systems [9,18]. We believe that the regime of instability reported here is intrinsically different from these earlier reports. The self-pulsing in the upper branch reported earlier arises due to a competition between the two time scales, one associated with the slow population transfer through optical pumping and the other involving fast variation of the optical nonlinearities, as explained in Refs. [9,17]. In our system the self-pulsing occurs at low input intensities, sometimes even lower than intensities associated with the bistable thresholds. Moreover, unlike earlier studies it does not require finite atom-field detuning or cavity detuning [19], and occurs without coupling to multiple modes of the cavity.

II. SYSTEM DESCRIPTION

We consider a unidirectional optical ring cavity of resonant frequency ω_o and total length $\mathcal{L}$. The active medium is confined within a length L and the transmissivity of the coupling mirrors is T, as shown in Fig. 1. The active medium consists of a closed atomic system in the Ξ (ladder) configuration, and couples to a weak probe (having frequency ω_p) and strong control field (having frequency ω_c) along the lower and upper transitions, respectively. Only the control field circulates in the cavity and exhibits a cooperative phenomenon as it

*hwanare@iitk.ac.in

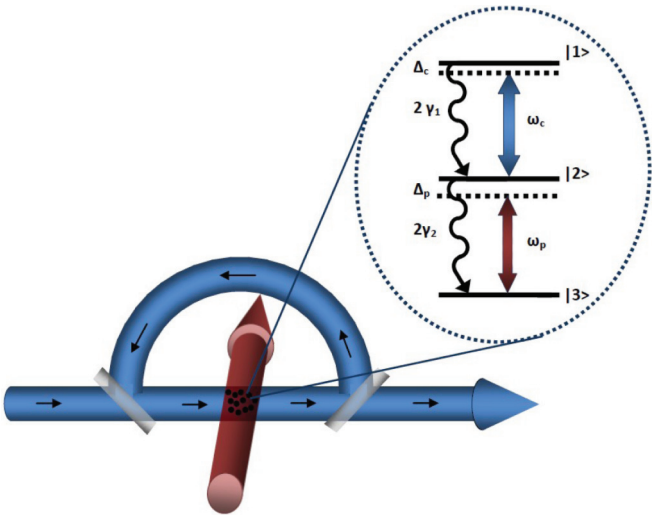

FIG. 1. (Color online) The probe field in red (thick vertical arrow) interacts with a collection of atoms whose susceptibility is dictated by the control field in blue (thin arrows) circulating in a cavity. Inset: The three-level ladder (Ξ) system and the associated fields.

experiences sufficient feedback provided by the cavity. The normalized cavity detuning with respect to control field is defined as $\delta_c = (\omega_o - \omega_c)\mathcal{L}/c$. For simplicity, we consider the OB phenomenon in the mean-field limit (i.e., $\alpha L \to 0, T \to 0$, such that $C = \alpha L/2T$ is finite) [14]. This ensures that the control field experiences weak absorption (α is the absorption coefficient along the upper transition) in a single traversal through the cavity and it undergoes many such round trips in the cavity, leading to a substantial interaction. Moreover, the field distribution remains spatially uniform throughout the active medium. Here the probe field is weak and thus couples to the atom linearly, whereas the atom-control field coupling OB is considered to all orders. However, we have not undertaken any such perturbative truncation and the results presented here were obtained from numerical simulations undertaken along the lines described in detail in Ref. [11].

We consider only the simplest configuration with regard to the atom-cavity coupling that captures the essential physics, where the atoms are homogeneously broadened, exhibiting radiative decay and they couple to a single mode of the cavity. The atom-field interaction is described by the density-matrix equation, Eq. (1), in the semiclassical regime, and the field dynamics are described by Eq. (2) obtained in the mean-field limit under a slowly varying envelope approximation, which captures the cavity feedback of the control field on the atoms through the cooperative parameter (C):

$$\frac{\partial \rho}{\partial t} = -\frac{i}{\hbar}[\hat{H}, \rho] + \hat{\mathcal{L}}\rho, \tag{1}$$

$$\frac{\partial x_c}{\partial t} = \kappa\left[-\left(1 + i\frac{\delta_c}{T}\right)x_c + y_c + 2iC\rho_{12}\right]. \tag{2}$$

The atom-field coupling and the atom-field detunings are contained in the total Hamiltonian $\hat{H} = \hbar[(\Delta_c + \Delta_p)|1\rangle\langle 1| + \Delta_p|2\rangle\langle 2| - (G_c|1\rangle\langle 2| + G_p|2\rangle\langle 3| + \text{H.c.})]$ in the dipole approximation after undertaking the rotating-wave approximation. The probe field coupling is given by the Rabi frequency $G_p = \vec{d}_{23} \cdot \vec{E}_p/\hbar$ and the detuning is $\Delta_p = \omega_{23} - \omega_p$, where $\vec{E}_p$ is the probe field amplitude. Similarly, we define G_c and Δ_c associated with the intracavity control field. The incoherent processes such as spontaneous emission decays ($2\gamma_i$) from the state $|i\rangle$, as shown in Fig. 1, are contained in the Liouville operator ($\hat{\mathcal{L}}$). The normalized cavity input and output strength of the control field are defined as $y_c = \vec{d}_{12} \cdot \vec{E}_c^{\text{in}}/(\hbar\kappa\sqrt{T})$ and $x_c = \vec{d}_{12} \cdot \vec{E}_c^{\text{out}}/(\hbar\kappa\sqrt{T})$, respectively. Here $\vec{d}_{12}$ is the dipole moment associated with the $|1\rangle \leftrightarrow |2\rangle$ transition and $\vec{E}_c^{\text{in(out)}}$ is the amplitude of the input (output) control field. All the frequency units are normalized with respect to the cavity decay κ, unless specified otherwise.

III. CONTROL OF SUSCEPTIBILITY

A. Normal and anomalous dispersion

The susceptibility experienced by the probe field can be obtained under two circumstances, depending on the specific state of the bistable control field. These bistable states correspond to either the cooperative (lower) branch or the one-atom (upper) branch of the S-shaped OB response. The refractive index and absorption are directly proportional to the real and imaginary parts of ρ_{23}, respectively, and their dependence on the probe detuning Δ_p is presented in Fig. 2. Note that the input control field strength ($|y_c|$) and its detuning (Δ_c) are held constant as the probe detuning (Δ_p) is varied. For the system in the lower OB branch (OFF state) the probe field experiences anomalous dispersion accompanied by an absorption peak at $\Delta_p/\kappa = 0$ [see Fig. 2(a)] with a resonant control field ($\Delta_c/\kappa = 0$). For the system in the upper branch (ON state) the probe field experiences normal dispersion accompanied with negligible absorption [see Fig. 2(b)]. Thus, depending on

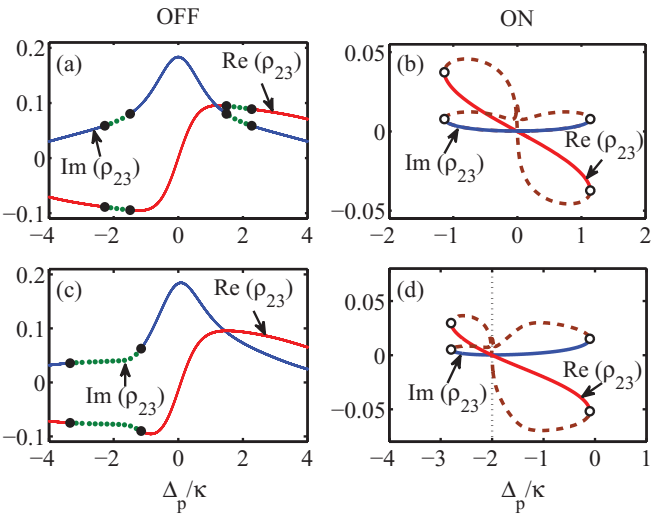

FIG. 2. (Color online) (a) The refractive index (red solid curve) and the absorption (blue solid curve) experienced by the probe field corresponding to the lower branch of OB and similarly (b) shows the probe susceptibility for the upper branch of OB with $\Delta_c/\kappa = 0$. (c) and (d) indicate the probe susceptibility for the detuned control field $\Delta_c/\kappa = 2$. The stable regions (solid) are separated from the unstable (green dotted or brown dashed) by the Hopf (H) and Limit points (LP) indicated with filled circles and open circles, respectively. The control field input $|y_c| = 3.0$, and the other parameters are $C = 200$, $|G_p|/\kappa = 0.2$, $\gamma_1/\kappa = 0.01$, $\gamma_2/\kappa = 1$, and $\delta_c = 0$.

the bistable ON or OFF state, the probe experiences normal or anomalous dispersion. Note that, with the negative sign for the probe frequency in the definition of the detuning ($\Delta_p = \omega_{23} - \omega_p$), the slope $\partial\rho_{23}/\partial\Delta_p > 0$ corresponds to anomalous dispersion and $\partial\rho_{23}/\partial\Delta_p < 0$ corresponds to normal dispersion. The probe response for finite control field detuning $\Delta_c/\kappa = 2$ is given in Figs. 2(c) and 2(d), wherein anomalous dispersion continues to occur at $\Delta_p \approx 0$ and normal dispersion to occur at $\Delta_p \approx -\Delta_c$.

Apart from obtaining the steady-state response of ρ_{23}, we have undertaken the linear stability analysis [20] where the eigenvalues of the Jacobian matrix of the system are examined to identify stable and unstable steady states and are indicated as red or blue solid curves and green dotted or brown dashed curves, respectively, throughout the paper. The physically inaccessible unstable states having eigenvalues with positive real and zero imaginary parts are shown as brown dashed curves. The regimes of nonlinear dynamical instability are indicated as green dotted curves. The steady-state response of ρ_{23} corresponding to the upper and middle branch of control field OB appears as a closed loop [Figs. 2(b) and 2(d)], where the regions associated with the dashed brown lines are inaccessible as they correspond to the usual unstable solution of the S-shaped OB curve. The system prepared in such a state would switch to the available ON or OFF state depending on the initial preparation. The spectral response for the lower branch OB is given in Figs. 2(a) and 2(c). We would like to point out that corresponding to each point in Fig. 2 (where a multiple response exists) one can obtain the associated conventional S-shaped OB response (Fig. 3) as the control field input strength is varied.

In order to understand the effects of the cavity feedback, we have compared the probe dispersion and absorption with the conventional response arising without feedback. In Figs. 4(a) and 4(b) the dash-dotted curves indicate the probe

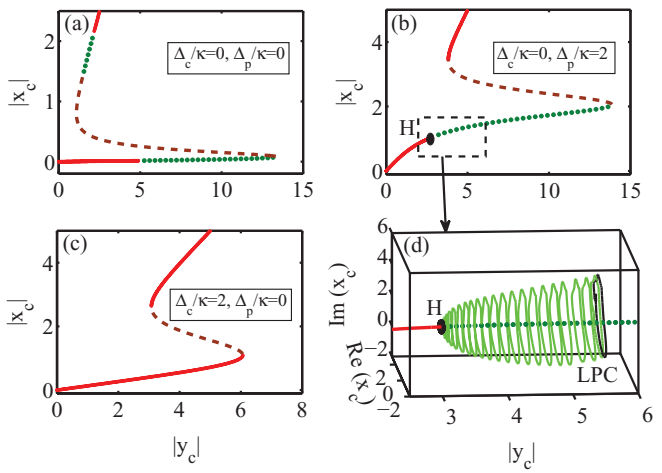

FIG. 3. (Color online) Optical bistable response of the control field as y_c is varied for various detunings. (a) $\Delta_c/\kappa = 0$, $\Delta_p/\kappa = 0$; (b) $\Delta_c/\kappa = 0$, $\Delta_p/\kappa = 2$; (c) $\Delta_c/\kappa = 2$, $\Delta_p/\kappa = 0$. The nonlinear dynamical regime is shown as green dotted curve. (d) The limit cycle continuation from the Hopf point (H) in (b) leads to periodic self-pulsing. The limit point of cycle (LPC) is indicated in black and self-pulsing does not occur beyond it. The other parameters are the same as in Fig. 2.

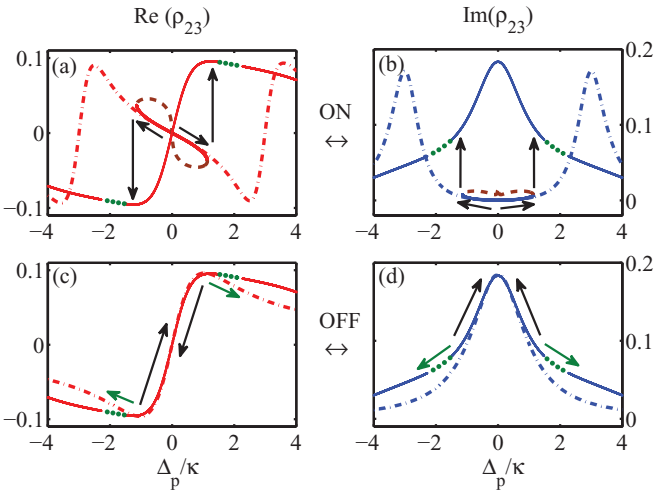

FIG. 4. (Color online) The switching of refractive index and absorption as the probe detuning is varied. (a) and (b) correspond to normal dispersion and indicate the switching from the ON to OFF state. (c) and (d) correspond to the OFF state exhibiting anomalous dispersion (black arrows). The green (light gray in grayscale version) arrows indicate the probe frequency variation leading to periodic self-pulsing. The dash-dotted lines correspond to response without feedback. The parameters are the same as in Fig. 2.

response without feedback for $|y_c| = |G_c|/\kappa = 3$, which is the intracavity value for OB in the upper branch, where an EIT-like profile is observed. The arrows indicate how the system switches from the upper branch to the lower branch as the probe detuning Δ_p is varied. In order to switch the associated dispersion from the normal to anomalous regime one needs to access the lower branch. This can be achieved by adiabatically changing the probe detuning beyond the turning points [Fig. 4(a)], wherein the system would jump to the lower OB state exhibiting anomalous dispersion [Fig. 4(c)] as the probe frequency is brought back into resonance.

The above response is consistent with the analytical results obtained in the perturbative limit of a weak probe field. The change in the slope of the dispersion is clear from the expression of the density-matrix element,

$$\rho_{23} = \frac{iG_p}{\left[\gamma_2 + i\Delta_p + \frac{|G_c|^2}{\gamma_1 + i(\Delta_c + \Delta_p)}\right]}. \tag{3}$$

The control field within the cavity dictates the probe response. For the absorptive OB case ($\Delta_c/\kappa = 0$), when the system is in the lower branch, the intracavity field would be weak due to the large collective absorption of the atoms which results in a conventional Lorentzian response for the probe field, as the $|G_c|^2$ term in Eq. (3) is negligible. However, when the system is in the upper branch, the term $|G_c|^2$ is dominant and the imaginary part of ρ_{23} becomes negligible. In the dispersive OB case ($\Delta_c/\kappa = 2$), it is apparent that the term $|G_c|^2$ becomes even more significant at the two-photon resonance, i.e., $\Delta_c + \Delta_p = 0$. This is clear from Figs. 2(c) and 2(d), wherein the upper branch response occurs only at the two-photon resonance, unlike for the system in the lower branch which continues to peak at the probe resonance $\Delta_p \approx 0$. The probe continues to experience anomalous dispersion at $\Delta_p \approx 0$ and normal dispersion at $\Delta_p \approx -\Delta_c$. The change in sign of

the dispersion profile is clearly seen in the derivative of ρ_{23} with respect to the detuning Δ_p, in the vicinity of $\Delta_p \approx 0$, and at $\Delta_p \approx -\Delta_c$ for the associated intracavity control field strength,

$$\frac{d\rho_{23}}{d\Delta_p} = \frac{G_p\left[1 - \frac{|G_c|^2}{\gamma_1 + i(\Delta_c + \Delta_p)^2}\right]}{\left[\gamma_2 + i\Delta_p + \frac{|G_c|^2}{\gamma_1 + i(\Delta_c + \Delta_p)}\right]^2}. \tag{4}$$

The complete bistable response arises from cavity feedback which is not included in the above analytical expression. In order to systematically include the cavity feedback that determines $|G_c|^2$ in the above equation, coupling to the atom through the density-matrix element ρ_{12} is essential [see Eq. (2)]. The term ρ_{12} itself involves a sixth-order polynomial of the intracavity field strength G_c. The determination of the intracavity control field is further complicated, as the OB response itself is dependent on the population excited by the probe field, hence a complete analytical expression is quite cumbersome. It should also be noted that the population is largely confined to the ground state $|3\rangle$, with only about 10^{-1}–10^{-2} in the excited states when the atom is in the lower branch of OB. For the atom in the upper branch, the steady-state populations of states $|1\rangle$ and $|2\rangle$ are about 10^{-4} and 10^{-6}, respectively. Moreover, in the upper branch the ratio of steady-state populations is related to the ratio of decay rates $\rho_{11}/\rho_{22} \propto \gamma_1/\gamma_2$. Such a three-level Ξ system could be realized in ^{85}Rb atomic vapor along the $5S_{1/2} \leftrightarrow 5P_{3/2} \leftrightarrow 5D_{5/2}$ transitions with a number density of $\sim 10^{17}$ atoms/m^3 and a spontaneous emission decay rate $\sim 10^7$ Hz, in a ring cavity with $T \sim 10^{-2}$, and the resulting cooperative parameter $C \sim 1000$. Inhomogeneous broadening arising from the Doppler effect can be canceled to first order by choosing the probe and control field beams to be counterpropagating within the active medium [21]. The input power levels for the bistable field $\sim$20 mW across a spot size of 100 μm would be sufficient for switching to the upper branch. The probe susceptibility and the associated group velocity are given as

$$\chi = \frac{3N\lambda_p^3}{8\pi^2}\left(\frac{\gamma_2\rho_{23}}{G_p}\right), \quad v_g = \frac{c}{n_g}, \tag{5}$$

where the group index $n_g = n + \omega_p(\partial n/\partial\omega_p)$. The relation between the refractive index (n) and the susceptibility (χ) is given by $n^2 = n_{\rm bg}^2 + \chi$, where $n_{\rm bg}$ is the background refractive index. Taking an atomic number density $N \sim 6 \times 10^{17}$ atoms/m^3, a spontaneous decay rate $\gamma_2 \sim 2 \times 10^7$ Hz, the wavelength of the probe laser $\lambda_p \sim 780$ nm, and $\partial\rho_{23}/\partial\Delta_p$ obtained from Figs. 2(a) and 2(b), results in a group index for both the anomalous and normal dispersion conditions as $\sim -15 \times 10^4$ and 4.3×10^4, respectively.

B. Periodic self-pulsing of refractive index

We now focus our attention to the effects of feedback of the control field which results in nonlinear dynamical self-pulsing. The probe response (solid) with the control field OB feedback digresses from the noncavity case (dash-dotted) for $|\Delta_p|/\kappa > \gamma_2/\kappa$, as seen in Fig. 4. We would like to emphasize that this difference arises from the feedback and lies at the heart of the periodic self-pulsing (the green dotted region) that the system exhibits in the lower branch.

The atomic system is chosen such that the uppermost state $|1\rangle$ is metastable and thus has a longer lifetime in comparison to the intermediate state $|2\rangle$. The stability of the lower bistable branch depends on the population injection by the probe field into the bistable transition. Such processes lead to the creation of instability in the lower bistable branch for appropriate probe detuning [see Figs. 3(a) and 3(b)]. This unstable regime is associated with oscillatory dynamics such as stable periodic self-pulsing [see Fig. 3(d)]. In our parameter regime, the oscillatory behavior does not necessarily occur between the lower and upper branches of the bistable response [19]. We believe that the physical mechanism involved in our system is intrinsically different from earlier reports of instability in the upper branch where optical pumping is invariably involved, which in turn relies on slow processes such as spontaneous emission [17]. In contrast, our system involves a competition between the population decay from the state $|2\rangle$ to the ground state $|3\rangle$ and nonlinear atom-field interaction along the $|1\rangle \leftrightarrow |2\rangle$ transition of the control field experiencing sufficient feedback. Atomic coherence is essential in obtaining the oscillatory behavior, and inclusion of larger decoherence of the atomic polarizations (ρ_{12} or ρ_{23}) leads to a reduction of the unstable range and its eventual disappearance. It should be noted that obtaining a bistable solution and the associated switching between the states is not essential for obtaining nonlinear dynamical self-pulsing in the lower branch, however, cavity feedback (cooperative effect) is mandatory. Furthermore, self-pulsing could occur at the very onset of the lower cooperative branch, thus requiring much lower input intensities in contrast to the conventional single-mode self-pulsing that occurs in the upper branch [22]. The concerns over power requirements can further be relaxed by implementing this scheme in photonic crystal-based microcavities which provide significant field enhancements [23] accompanied by short cavity round-trip times.

The self-pulsing domain associated with the unstable solutions are separated from the stable solutions by a Hopf (supercritical) point, as indicated in Fig 2. The limit cycles

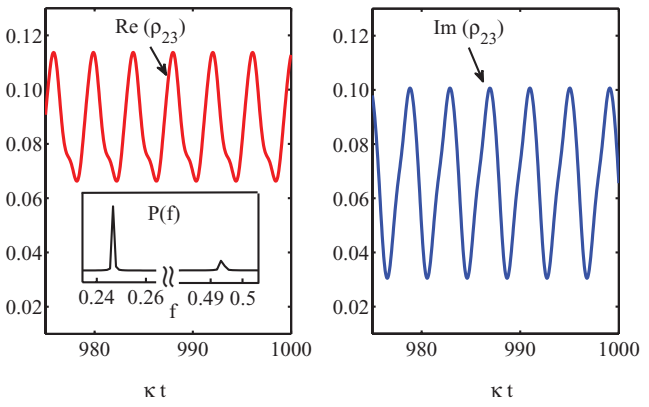

FIG. 5. (Color online) The time-periodic self-pulsing of the real and imaginary parts of ρ_{23} and the power spectral density (inset) is shown for $\Delta_p/\kappa = 2$, $|y_c| = 3$, $G_c/\kappa = 0.2$, and all the other parameters are the same as in Fig. 2.

that originate from the Hopf points are robust and stable. The Floquet analysis indicates that the Floquet multipliers are bound by unity, within this range of detunings, leading to stable limit cycles [24]. The stable periodic oscillations occur for both the absorption as well as the refractive index (see Fig. 5). The observed modulation in the refractive index and the absorption is of the order of 3% and 7%, respectively. These oscillations are not necessarily sinusoidal, and one can obtain a variety of multiply peaked periodic oscillations with varied frequency content. The self-pulsing time scale is governed by the cavity decay time $\kappa^{-1} = \mathcal{L}/cT$. In our simulations the atomic states are long lived in comparison to cavity decay times, and in order to realize this phenomenon, these can be chosen to have a variety of values satisfying the condition $\gamma_1 \ll \gamma_2 \leqslant \kappa$. In particular, for a microcavity setup we consider $\gamma_1/\kappa \sim 10^{-7}$, $\gamma_2/\kappa \sim 10^{-5}$, $L \sim 10^{-6}$ m, $T \sim 10^{-2}$, $C \sim 20$, and obtain similar self-pulsing, wherein $\kappa \sim 10^{12}$ Hz and thus periodic self-pulsing in the terahertz regime seems possible in this OB setups, with a constant input field y_c.

IV. SUMMARY

In conclusion, we have demonstrated a coherent way to engineer refractive index (normal to anomalous) and absorption of a probe field using OB. Such OB in multilevel systems can be used as optical delay lines for the control of pulse propagation in integrated optical devices. Furthermore, we also demonstrate a mechanism to obtain time-dependent oscillatory susceptibility, with a constant input control field, operating in the lower cooperative branch of OB. A distinct possibility of exploiting this scheme to obtain refractive index modulation in the terahertz regime needs to be tested, as the conventional slow dynamics associated with optical pumping is no longer a limiting factor in our scheme.

[1] L. V. Hau, S. E. Harris, Z. Dutton, and C. H. Behroozi, Nature (London) **397**, 594 (1999).

[2] L. J. Wang, A. Kuzmich, and A. Dogariu, Nature (London) **406**, 277 (2000).

[3] S. E. Harris, Phys. Today **50**(7), 36 (1997).

[4] M. O. Scully, Phys. Rev. Lett. **67**, 1855 (1991).

[5] S. Chakrabarti, S. A. Ramakrishna, and H. Wanare, Opt. Express **16**, 19504 (2008).

[6] C. O'Brien and O. Kocharovskaya, Phys. Rev. Lett. **107**, 137401 (2011).

[7] C. O'Brien, P. M. Anisimov, Y. Rostovtsev, and O. Kocharovskaya, Phys. Rev. A **84**, 063835 (2011).

[8] W. Harshawardhan and G. S. Agarwal, Phys. Rev. A **53**, 1812 (1996).

[9] H. Wang, D. J. Goorskey, and M. Xiao, Phys. Rev. A **65**, 011801 (2001).

[10] H. A. Babu and H. Wanare, Phys. Rev. A **83**, 033818 (2011).

[11] H. A. Babu and H. Wanare, Phys. Rev. A **83**, 033819 (2011).

[12] W. Yang, A. Joshi, and M. Xiao, Phy. Rev. Lett. **95**, 093902 (2005).

[13] A. Joshi and M. Xiao, J. Mod. Opt. **57**, 1196 (2010).

[14] L. A. Lugiato, *Progress in Optics*, edited by E. Wolf (North-Holland, Amsterdam, 1984), Vol. XXI, p. 69.

[15] H. M. Gibbs, *Optical Bistability: Controlling Light with Light* (Academic, Orlando, FL, 1985).

[16] K. Ikeda, Opt. Commun. **30**, 257 (1979); K. Ikeda, H. Daido, and O. Akimoto, Phys. Rev. Lett. **45**, 709 (1980).

[17] A. Lambrecht, E. Giacobino, and J. M. Courty, Opt. Commun. **115**, 199 (1995).

[18] W. Yang, A. Joshi, and M. Xiao, Phys. Rev. A **70**, 033807 (2004).

[19] H. J. Carmichael, Phy. Rev. Lett. **52**, 1292 (1984).

[20] Y. A. Kuznetsov, *Elements of Applied Bifurcation Theory* (Springer, New York, 1998).

[21] J. Gea-Banacloche, Y. Q. Li, S. Z. Jin, and M. Xiao, Phys. Rev. A **51**, 576 (1995).

[22] L. A. Lugiato, R. J. Horowicz, G. Strini, and L. M. Narducci, Phys. Rev. A **30**, 1366 (1984).

[23] J. Bravo-Abad, A. Rodriguez, P. Bermel, S. G. Johnson, J. D. Joannopoulos, and M. Soljacic, Opt. Express **15**, 16161 (2007).

[24] S. H. Strogatz, *Nonlinear Dynamics and Chaos* (Perseus, New York, 1994).